J. Membrane Biol. 72, 161–171 (1983)

The Journal of
Membrane Biology

The Band 3-Rich Membrane of Llama Erythrocytes: Studies on Cell Shape and the Organization of Membrane Proteins

Jena K. Khodadad and Ronald S. Weinstein

Departments of Anatomy and Pathology, Rush Medical College and Rush-Presbyterian-St. Luke's Medical Center, Chicago, Illinois 60612

Summary. The erythrocyte membrane of the llama was characterized in comparison to that of the human. The llama erythrocyte was an elliptical disk that resisted shape alterations in hyperosmotic buffers and following metabolic depletion, both of which induce spiculation of the human red cell. Lysophosphatidylcholine incorporation produced minor serrations of the edge of the llama disk but no spicules, whereas human red cells became sphero-echinocytes. The polypeptide profiles in the membranes of the two species were similar, except for several noteworthy differences: a marked elevation in the relative content of band 3; the absence of membrane-bound band 6; and simpler glycoprotein pattern in the llama. The concentration of band 3 in llama was about two and a half to three times that in the human and intramembrane particles in the protoplasmic leaflet of freeze-fractured llama membrane were correspondingly increased. The selective solubilization of bands 1, 2 and 5 in low ionic strength buffer, and all of the peripheral proteins in high alkaline buffer were similar except for increased retention of ankyrin by the llama membrane. These data suggest a similar disposition of membrane proteins. The llama membrane was markedly resistant to the solubilization of integral proteins by the nonionic detergent, Triton X-100. This property and the general resistance to shape changes may be related to the high concentration of band 3.

Key Words erythrocytes · membranes · llama · organization · proteins · band 3 · cell shape · deformability

Introduction

A classical approach to understanding structure/function relationships in biological systems is through the comparison of variations among selected species. The erythrocytes of the human and llama are such a pair. Human erythrocytes are biconcave disks and are readily deformed by shear stress (Schmid-Schonbein & Wells, 1969), whereas llama erythrocytes are elliptical disks and are resistant to hydrodynamically induced shape alterations (Smith, Mohandas & Shohet, 1979). In these respects, llama erythrocytes are similar to a related species, the camel (Smith et al., 1979). Camel erythrocytes have far greater mechanical and osmotic durability than the human erythrocytes (Perk, 1963; Perk, Frei & Herz, 1964; Livne & Kuiper, 1973; Yagil, Sod-Moriah & Myerstein, 1974), and llama erythrocytes are more resistant to hypotonic solutions than human red cells (Reynafarje et al., 1975). In this study, we present the first analysis of the polypeptides of the membrane of the llama erythrocyte and correlate these data with the ultrastructure and shape behavior of the membrane. A preliminary account of this work has been published (Khodadad & Weinstein, 1980).

Materials and Methods

Blood was obtained from unsedated llamas (*Llama glama*) and normal human donors by venipuncture, using sodium heparin or EDTA as the anticoagulant. Unless otherwise stated, all procedures were carried out on fresh samples of blood at 0 to 5 °C and all centrifugations were done in a Beckman Model J 2–21 centrifuge. Samples were initially washed three times in phosphate-buffered saline (PBS): 150 mM NaCl – 5 mM NaPi (pH 7.4). Ghosts were prepared in 5 mM NaPi (pH 8.0) as described by Fairbanks, Steck and Wallach (1971).

Enzymes, lysophosphatidylcholine, and dessicated firefly tails were obtained from Sigma. Chemicals were reagent grade or better and were obtained from Fisher or Sigma. Molecular weight standards were obtained from Biorad.

Morphological Studies

Scanning Electron Microscopy. Erythrocytes were fixed in 2% glutaraldehyde in PBS, washed twice in deionized water and spread on a glass slide. Smears were air dried at room temperature and then in vacuo at 10^{-3} Torr overnight. Smears were coated with gold-palladium (60:40) in a Kinney Vacuum Evaporator, Model KDTG-3P and photographed with JEOL JSM-3SC scanning electron microscope, operated a 25 kV with the stage at either a 30° or 0° tilt angle.

Transmission Electron Microscopy. For thin-section electron microscopy, erythrocytes were fixed in 1% glutaraldehyde in PBS, postfixed in 1% osmium tetroxide in same buffer (one hour at room temperature), dehydrated through graded ethanol solutions, and embedded in Epon 812. Thin sections were prepared with LKB Ultrome III, mounted on grids, and stained with uranyl acetate and lead citrate. Micrographs were taken on

a Philips EM-301 transmission electron microscope at an accelerating voltage of 80 kV. For freeze-fracture electron microscopy, erythrocytes were fixed in 1% glutaraldehyde, washed in distilled water, suspended in 20% glycerin, and rapidly quenched in Freon 22 to −150 °C. Freeze-fracture and freeze-etch procedures were done in a Balzer's Model BAF 301 device by the method of Moor and Mühlethaler (1963). For deep etching, the stage temperature was maintained at −100 °C for 60 to 90 sec. Samples were replicated with platinum-carbon for one second at a 45° angle followed by carbon coating for 10 to 12 sec. Rotary shadowing (Margaritis, Elgsaeter & Branton, 1977) was at 25° angle with a Balzer's rotary shadowing unit. Replicas were floated on 0.9% saline, cleaned with Chlorox, rinsed in distilled water, and collected on 100 mesh copper grids. Replicas were photographed with a Philips 301 electron microscope.

Quantitative Analysis of Intramembrane Particles

Quantitative analyses of particle numerical densities were done on electron micrographs of rotary-shadowed replicas of fixed and glycerinated membranes at a final magnification of 250,000×. For quantitation a 10×10 cm transparent grid was superimposed on each micrograph and particles within that area were counted. Particle counts were done on ten cells in each category.

Surface Area

The surface of the llama erythrocyte was estimated from scanning electron micrographs. The major and minor axes of the llama elliptocytes were determined directly from scanning electron micrographs of 40 consecutive red cells photographed *en face* at 0° tilt angle at a calibrated magnification of 4,800. Estimates of thickness of llama elliptocytes were made by measuring the profiles of cells lying fortuitously on edge. The model of llama red cell was constructed from three elliptical, mutually perpendicular cross-sections. The values for the major and minor axes of these three ellipses were obtained from measurements on SEM. The contour of the perimeter of elliptocytes were determined from thin sections. Based on these data, a model of llama erythrocyte was constructed and the surface area of the model was estimated. For comparison the diameter of 25 consecutive human red cells prepared under similar conditions were measured directly from SEM.

Biochemical Procedures

Polyacrylamide gel electrophoresis and molecular weight estimates were performed as described (Fairbanks et al., 1971). Extraction with alkali was done according to Steck and Yu (1973).

Binding of Glyceraldehyde 3-Phosphate Dehydrogenase. Binding of G3PD to the membranes of llama and human erythrocytes was done according to the method of Kant and Steck (1973). Hemoglobin-free unsealed ghosts were prepared and depleted of the enzyme by incubation with 40 volumes of PBS for 20 min and then washed twice with the same buffer and three times with 5 mM NaPi, pH 8.0. Binding studies were done with the rabbit muscle enzyme using a 2 mg/ml solution in 5 mM NaPi, pH 8.0.

ATP Assay. Red cells were washed three times in 150 mM NaCl-5 mM NaPi, pH 7.4, and lysed in two volumes of boiling distilled water. Samples were used for hemoglobin determination and other samples were quickly frozen for ATP assay. The assay was done according to the method of Strehler and McElroy (1968) using dessicated firefly tails and a Farrand Mark IV fluorometer. Results were expressed in μg of ATP/g of hemoglobin.

Uptake of Lysophosphatidylcholine (LPC). Uptake of LPC by red cells was measured as described (Lange & Slayton, 1982). Data on uptake of radiolabeled LPC were expressed in terms of μg/cell.

Ghost counts were done using a Model A Coulter Counter (100 μ aperture) and corrected for coincidence.

Erythrocyte Shape Modification

Osmolarity. Approximately 0.2 ml of the washed packed cells were incubated for 30 min or 2 hr in 10 ml of 5 mM Na phosphate buffers (pH 7.4) containing sodium chloride to yield solutions with the following osmotic activity: 290, 500 and 700 mOsm. Aliquots of erythrocytes incubated first in 500 or 700 mOsm buffers, were subsequently incubated in buffers of 290 mOsm values, at room temperature for 30 min. Control cells were incubated throughout in a 290 mOsm buffer.

ATP Depletion. Metabolic depletion of cells was performed according to modification of the method of Weed, LaCelle and Merrill (1969). Cells were washed with 150 mM NaCl−5 mM NaPi buffer, pH 7.4, under sterile conditions with 1 μg/ml of streptomycin and 100 U/ml of penicillin and incubated over 26 hr at 37 °C. Adenosine (80 μg/ml of sample) was added to two sets of tubes: at the beginning of the first incubations in order to prevent metabolic depletion of cells or to the already depleted cells in order to replenish intracellular ATP content (Weed et al., 1969). The latter samples were reincubated for at least 4 hr at 37 °C. Aliquots of each sample were used for ATP assay.

Lysophosphatidylcholine (LPC) Treatment. Red cells were incubated for 20 min at either 25 or 0 °C in 19 volumes of 150 mM NaCl−5 mM NaPi buffer (pH 7.5) containing 0.1% bovine serum albumin and, 20 μg/ml of LPC (Marikovsky, Brown, Weinstein & Wortis, 1976) and 0.05 μCi of ^{14}C LPC. Aliquots were fixed in glutaraldehyde and used for electron microscopy. Other aliquots were used for determinations of LPC uptake.

Results

Morphology

Whereas human erythrocytes are biconcave disks, llama erythrocytes were observed to be elliptical disks (Fig. 1*a*). The llama red cells show increased thickness in the central region in contrast to human erythrocytes which showed two central depressions.

In thin sections, the cytoplasmic compartments of llama and human erythrocytes contained no organelles or formed structures and were uniformly electron dense, suggesting that hemoglobin was homogeneously distributed.

By SEM the glutaraldehyde-fixed air-dried human erythrocytes measured 6.8±0.4 (SD) μm in diameter. Llama erythrocytes measured

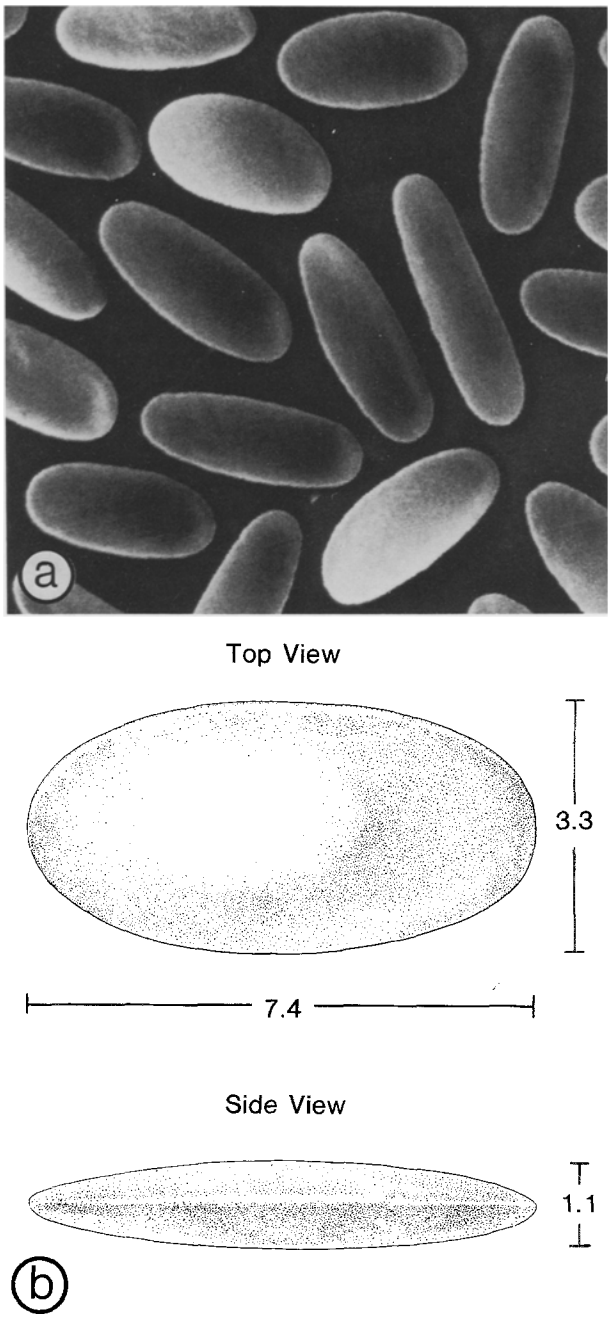

Fig. 1. Llama red cell. (*a*) SEM of llama RBCs demonstrate their elliptical shapes. Magnification 4,000×. (*b*) Diagrammatic model of the llama erythrocyte. Dimensions are in micrometers on fixed, air dried cells

7.4 ± 0.59 (SD) μm in maximum length and 3.3 ± 0.28 (SD) μm in greatest width and approximately 1.1 μm in thickness (Fig. 1*b*). From these dimensions, a model of the llama erythrocyte was constructed based on three elliptical, mutually perpendicular cross-sections for the purpose of estimating the surface area of the cell. One of the ellipses had major axis of 7.4 μm and minor axis of 3.3 μm; the curvature of this ellipse was determined from measurements on curvatures of twenty cells viewed *en face* on SEM and satisfied the relationship of the sums of the distances from any point on the curve to the two foci of an ellipse being equal (Considine, 1976). The second ellipse had a major axis of 7.4 μm and minor axis of 1.1 μm, and also satisfied the conditions for curvature of an ellipse as determined from measurements done on curvature in thin sections on twenty elongated profiles measuring over 6.5 μm in the major axis and under 1.5 μm in the minor axis. The third ellipse had the major axis of 3.3 μm and minor axis of 1.1 μm. Formulas analogous to those published for the human erythrocytes (Ponder, 1948) are not available for the llama. Therefore, surface area was determined experimentally using this model. The surface of the model was covered with nonstretchable but pliable onion skin paper and the area was determined by weighing the surface cover. Five such determinations were done. A surface area of 43.4 ± 0.9 (SD) μm^2 was obtained.

Thin Sections. Cross-sectioned profiles of thin-sectioned erythrocyte membranes were similar in the llama and human. The thickness of the double dense lines of the unit membrane in the llama was approximately 70 Å, similar to that of the human erythrocyte membrane (Robertson, 1959).

Quantitation of Intramembrane Particles. Freeze-fracture of the erythrocyte membrane revealed two fracture faces bearing particles of different size and numerical density. In both human and llama, the particles were neither aggregated nor in another detectable pattern. P-face particles were represented in greater numbers than E-face particles. There was a higher numerical density of particles on the P-face of llama erythrocytes (Fig. 2*b*) when compared to the human (Fig. 2*a*). Quantitative analysis of rotary-shadowed replicas revealed 5400 ± 340 (SD) P-face particles per μm^2 in the llama and 2500 ± 270 (SD) P-face particles per μm^2 in the human; this difference being statistically significant ($p < 0.001$). In contrast, the numerical density of particles at the E-face of llama was slightly less than that of the human: 191 ± 57 (SD) in llama versus 225 ± 83 (SD) per μm^2 of membrane in the human (Fig. 2*c*, *d*). Using 138.1 μm^2 (Canham & Burton, 1968) and 43.4 μm^2 as values for surface areas of membranes of the human and llama red cells, respectively, it was estimated that there are 3.45×10^5 P-face particles per human and 2.34×10^5 P-face particles per llama erythrocyte. It is clear from these numbers and from Fig. 2 that the increase in the numerical density of the proto-

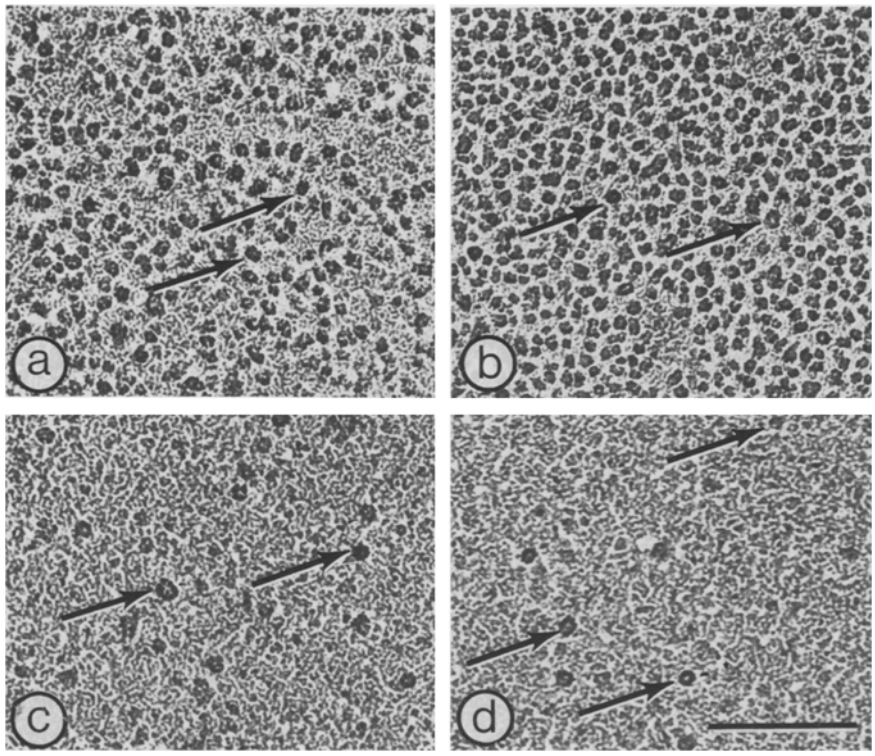

Fig. 2. Freeze-fractured membranes. Replicas of freeze-fractured glutaraldehyde-fixed and glycerinated red blood cells, rotary shadowed at 25° angle. Magnification 200,000×. 0.1 μm = bar. (*a*+*b*) P-fracture faces of human and llama cells, respectively. The P-face particles (arrows) are more abundant in llama membrane (*b*) than the human (*a*). (*c*+*d*) E-fracture faces of human and llama RBCs. The particles (arrows) are slightly decreased in numbers in the E-face of llama membrane (*d*) when compared to that of the human (*c*)

plasmic leaflet intramembrane particles of the llama membrane cannot be attributed to a differential partitioning from the exoplasmic leaflet.

Biochemical Characterization

The weight ratio of protein to phospholipid was 3.32 in llama and 1.87 in human erythrocyte membranes (Table). The molar ratio of cholesterol to phospholipid was similar in the two species (Table): 0.79 for the human and 0.76 for the llama.

Electrophoretograms of SDS solubilized membrane proteins on polyacrylamide gels showed a close similarity of the major polypeptides in the human and llama erythrocyte membranes (Fig. 3). Thus, spectrin (bands 1 and 2), ankyrin (band 2.1 seen as a shoulder on the leading edge of band 2), actin (band 5), and bands 3, 4.1, 4.2, and 7 were present in the llama as in the human (*see* Steck, 1974). However, there were characteristic differences in the membrane preparations. Llama membranes evinced a band of the molecular weight of globin; this reflects the fact that llama ghosts remained pink (i.e. were more resistant to complete hemoglobin removal under conditions which elute all hemoglobin from human erythrocyte membranes). Extra bands were also observed migrating ahead of band 5 in the llama. We do not believe that these correspond to band 6 which in humans represents glyceraldehyde-3-P dehydrogenase, since the ghosts lacked this enzyme activity.

Most notably, band 3 showed slower electrophoretic mobility and greater abundance in the llama where it constituted approximately 36% of the total membrane protein in contrast to 24% in the human (Steck, 1974). Its apparent molecular weight was 98,000 dalton in the llama and 88,000 in human; this value for the human compares with the estimated molecular weight of 88,000–95,000 daltons reported (Steck, 1978). The densitometric tracing of llama band 3 was also sharper, more symmetrical and monodisperse than that of the human.

Prevalence of Band 3. Densitometric integration and molecular weight estimates of the band 3 polypeptide gave an estimate of 1.0×10^6 copies of band 3 protomers per llama erythrocyte. This is indistinguishable from the value of 1.0×10^6 to 1.2×10^6 copies in the human erythrocyte membranes (Guidotti, 1972; Steck, 1974; Steck, 1978). Based on surface areas of 43.4 and 138.1 μm^2, respectively, for human and llama red cells, the band 3 protomer is approximately three times more concentrated in the llama.

Glycoproteins. The elctrophoretograms obtained from periodic acid-Schiff (PAS)-stained polyacrylamide gels of SDS-solubilized membranes differed

Table 1. Chemical characterization of membranes

Species	Sialic acids[a]		Protein/ Phospho-lipid[b] (mg/mg)	Cholesterol/ Phospholipid[c] (mole/mole)
	Per μm² (μmoles $\times 10^{-13}$)	N'ase sensitive (%)		
Human	4.5	83	1.87	0.79
Llama	5.8	53	3.32	0.76

[a] Sialic acid was determined by modification (Tischer & Peters, 1965) of the method of Warren (1959). Total sialic acid determination was preceded by hydrolysis at 80 °C for 1 hr in 2 N H_2SO_4. Neuraminidase treatment of cells was with neuraminidase from *Clostridium perfringens*. The reaction mixture contained 1.6×10^6 red cells, 50 μg of neuraminidase, 0.005 Tris acetate, 0.01 NaCl (pH 5.7). Incubations were at 37 °C for 30 min. Samples were centrifuged and the supernatant was assayed for sialic acid. Values are averages of close data from triplicate experiments. The amount of sialic acid was 6.27×10^{-11} μmoles per human and 2.89×10^{-11} μmoles per llama red cell. The calculations of sialic acid per unit of membrane was based on the values of 138.1 μm² (Canham & Burton, 1968) and 43.4 μm², as described in text, for the surface areas of human and llama red cell, respectively.

[b] Protein was determined (Lowry, Rosebrough, Farr & Randall, 1951) with crystalline bovine serum albumin as standard. Results were determined per red cell based on cell counts obtained with a Coulter counter. There were 4.9×10^{-10} mg of protein per llama and 5.5×10^{-10} mg of protein per human red cell (*see also* Dodge, Mitchell & Hanahan, 1963 and Fairbanks et al., 1971). Phospholipid phosphorus was determined following extraction with 2:1 chloroform/methanol (Folch, Lees & Sloane-Stanley, 1957) according to Ames (1966). Protein and phospholipid values are averages of close data from triplicate experiments.

[c] Membrane cholesterol and phospholipid content was determined in lipids extracted from ghosts (Folch et al., 1957). Cholesterol content was determined as described by Parekh and Jung (1970) and phospholipid according to Gomori (1942). Results were expressed as molar ratios of cholesterol to phospholipid. Values are averages of close data on duplicate experiments.

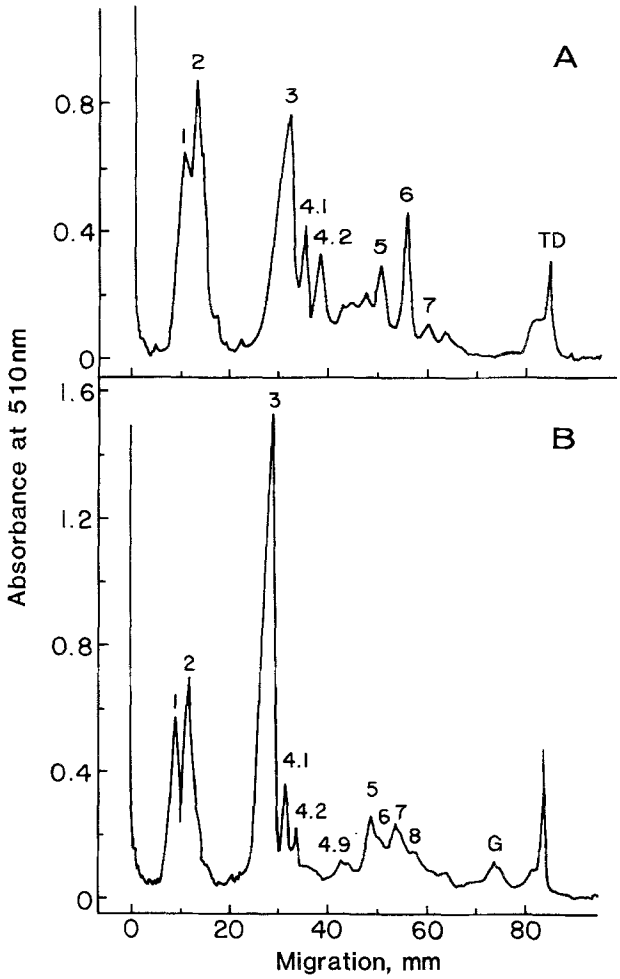

Fig. 3. Densitometric scans of Coomassie Blue-stained gels of membranes of the human (*A*) and the llama (*B*) erythrocytes. Forty μg of protein solubilized in SDS were loaded on gels. *TD* marks the position of the tracking dye; *G* is globin

markedly between llama and human (Fig. 4). Bands in the PAS-1 and PAS-2 mobility regions of human were absent in llama; instead, there was a prominent band in the PAS-3 position. Since considerable sialic acid is present in the llama membranes (Table) and this sugar is known to be particularly reactive to PAS staining, and because Fig. 4, panel *B* showed that most of the stain was in the protein peak and not in the lipid region (at the position of the tracking dye), we inferred that the peak in Fig. 4*B* is a (sialo)glycoprotein. There is also a minor band with the mobility of band 3. Whether it corresponds to band 3 is uncertain.

Sialic Acid. Total sialic acid per unit area of membrane was higher in llama than in human, whereas neuraminidase-sensitive sialic acid was lower in the llama (Table). Of the total sialic acid of the llama erythrocyte, 53% was susceptible to the action of neuraminidase, whereas in the human the neuraminidase-sensitive neuraminic acid constituted over 83% of the total sialic acid.

Solubilization of Membrane Proteins

Effects of Ionic Perturbation. The polypeptides of llama and human were stable in their association with the membrane in the presence of the isolation buffer, 5 mM NaPi, pH 8.0 (Fig. 5, gels 5–8). Incubation of ghosts at 37 °C for 15 min in seven volumes of 0.1 mM EDTA eluted bands 1, 2 and 5 from human (Fairbanks et al., 1971; *see* Fig. 5, gels 9 & 10) and most of bands 1, 2 and all of band 5 from the llama (Fig. 5, gels 11 & 12). Comparison of densitometric scans on gels obtained

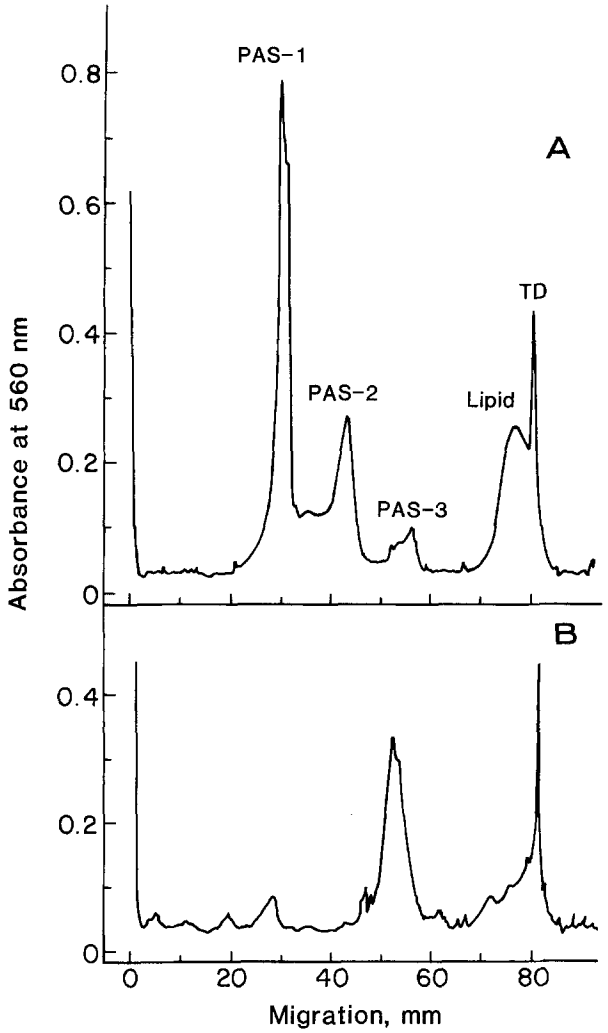

Fig. 4. Densitometric scans of membranes of the human (*A*) and the llama (*B*) erythrocytes after polyacrylamide gel electrophoresis and periodic-acid Schiff staining (Fairbanks et al., 1971). Scans were on duplicate gels obtained as in Fig. 3

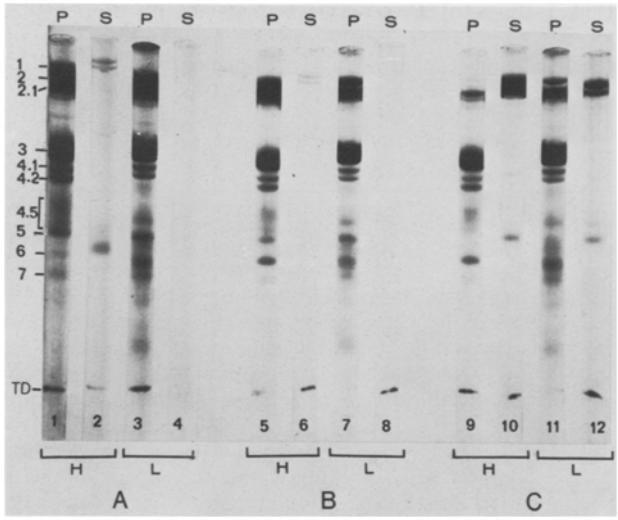

Fig. 5. Effect of the ionic milieu on the release of polypeptides from membranes. One volume (40 μg of protein) of human (*H*) or llama (*L*) ghost was suspended in seven volumes of: (*A*) phosphate-buffered saline (150 mM NaCl—5 mM sodium phosphate buffer, pH 8.0; (B) Na phosphate buffer (5 mM; pH 8.0); and (*C*) 0.1 mM EDTA, pH 8.0. The mixtures were incubated for 15 min at 37 °C (Fairbanks et al., 1971). The suspensions were then centrifuged and pellet (*P*) and supernatant (*S*) fractions analyzed by SDS polyacrylamide gel electrophoresis followed by staining with Coomassie blue

from pellet and supernatant fractions of llama ghosts treated with 0.1 mM EDTA (*see* Fig. 5, gels 11 & 12) shows that band 2.1 (ankyrin), the fraction migrating in the leading edge of band 2, remains associated with the llama membrane. Extraction with 150 mM NaCl—5 mM phosphate buffer at pH 8.0 eluted band 6 (glyceraldehyde 3-P dehydrogenase) from the human (Fairbanks et al., 1971; *see* Fig. 5, gel 2) but no proteins (Fig. 5, gel 4) or (sialo)glycoproteins (*not shown*) from the llama membranes. The membranes may lack G3PD or this enzyme may be lost during membrane preparation. Data on the binding of glyceraldehyde-3-P dehydrogenase demonstrate that llama red cells have a considerable capacity to bind G3PD although less than that of the human. The

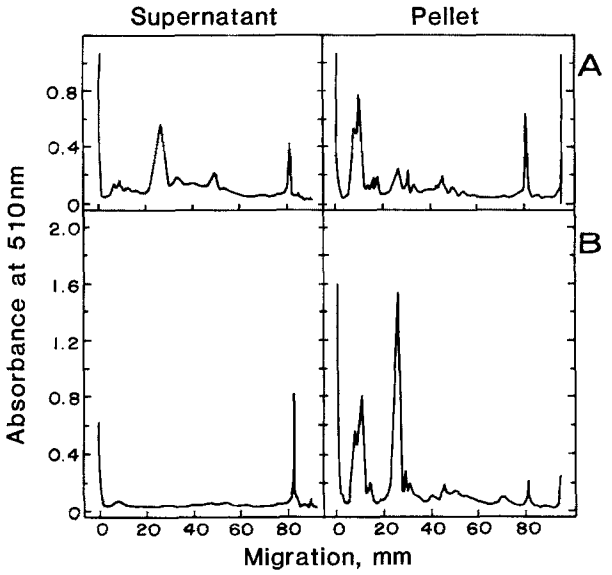

Fig. 6. Extraction of the membrane proteins with the nonionic detergent, Triton X-100. Ghost volumes equivalent to 40 μg of protein were incubated in 0.5% Triton X-100 in 5 mM sodium phosphate buffer, pH 8.0, for 20 min at 0 °C (Yu et al., 1973). Pellets and supernatants were solubilized in SDS and used for polyacrlyamide gel electrophoresis. Gels were stained with Coomassie Blue and scanned. Panel (*A*), human; panel (*B*), llama

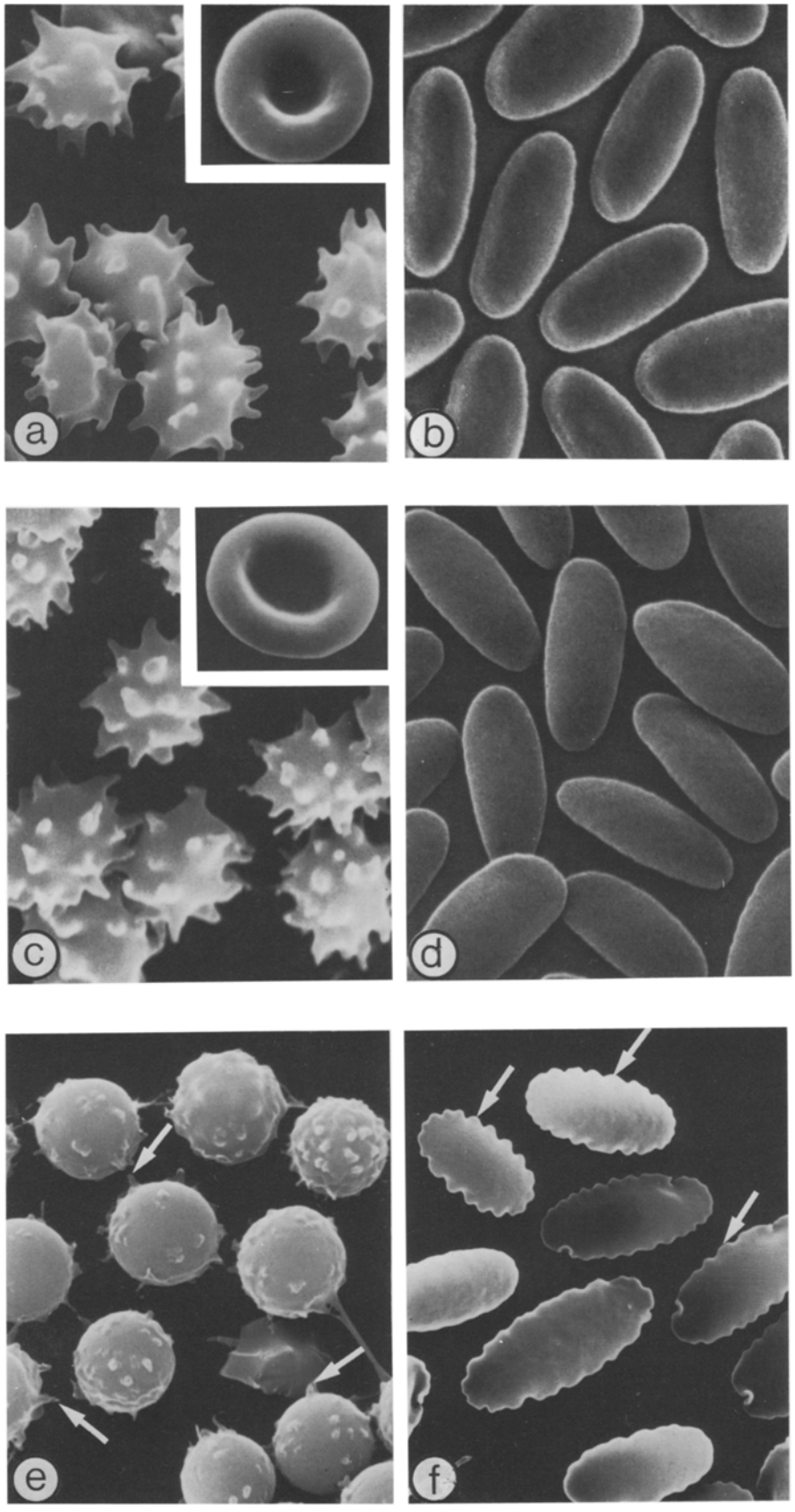

Fig. 7. Effect of osmotic factors, metabolic depletion, and lysophosphatidylcholine on the shapes of human and llama red cells. Magnifications 4,000×. (*a*+*b*) Effect of osmotic factors on shapes of red cells. (*a*) Incubations in presence of buffer with the osmotic potential of 500 mOsm results in the crenation of the human red cells; the normal biconcave disk shape is restored after incubation of these crenated cells in isosmotic buffer (insert). (*b*) Incubation of the llama red cells in buffer with osmotic potential of 700 mOsm leaves the shapes of the red cells essentially elliptical. (*c* & *d*) Effect of metabolic depletion on the shapes of the red cells. (*c*) Metabolic depletion of the human red blood cells results in crenation of the discocytes. Restoration of intracellular ATP restores the biconcave disk shape (insert). (*d*). Metabolic depletion of the llama red cells does not result in the shape alteration of these cells. (*e* & *f*) Effect of lysophosphatidylcholine on the shapes of red cells. (*e*) Incubation in presence of 20 μg/ml of lysophosphatidylcholine results in shape alteration of the human discocytes into sphero-echinocytes. These cells have long and pointed spicules (arrows). (*f*) Incubation in presence of 20 μg/ml of lysophosphatidylcholine results in the serration of the llama red cell membrane. These irregularities appear as blunt protrusions from the surface (arrows)

llama ghost binds $5.8 \times 10^5 \pm 0.09$ (SD) and the human $9.0 \times 10^5 \pm 0.18$ (SD) molecules of G3PD. If the enzyme associates with band 3 as in the human ghost binds (Yu & Steck, 1975) the higher concentration of band 3 in the llama membranes could interfere with its binding.

Alkali Treatment. Alkaline media, like other denaturing treatments, stripped human ghosts of all peripheral proteins, leaving associated with the lipid bilayer only the integral proteins (Steck & Yu, 1973). Thus, extraction at pH 12 or 13 solubilized bands 1, 2, 2.1, 4.1, 4.2, 5 and 6 from human ghosts but not band 3. Findings were similar for the llama (*not shown*). In the llama, similar to the human, the PAS positive band remains associated with the lipid bilayer. In the llama this PAS positive band corresponds in mobility to the band 7 polypeptide (*see* Fig. 4, panel *B*).

Effect of the Nonionic Detergent. Triton X-100 dissolved the bilayer and the proteins imbedded therein in human ghosts while spectrin, actin and band 4.1 remained associated as a filamentous network or reticulum (Yu, Fischman & Steck, 1973). Under identical conditions, ghosts from llama erythrocytes were resistant to this detergent. Band 3 was not extracted (Fig. 6, panel *B*) and only 68% of the major PAS-positive (sialo)glycoprotein was removed (*not shown*).

Shape Modification Studies

Hyperosmotic Effects. Exposure to hyperosmotic media caused human erythrocytes to shrivel osmotically from normal biconcave disks into spiculated cells (Fig. 7*a*); this process was reversible upon reincubation of these cells in isosmotic medium (Marikovsky, Khodadad & Weinstein, 1978, *see* Fig. 7*a*, insert). This change in contour was not observed in the llama erythrocytes. The llama erythrocytes did not crenate after exposure to media with osmotic activity of 700 mOsm over incubation periods of 30 min (Fig. 7*b*) and even up to several hours. The shape of these cells remain unchanged after their subsequent incubation in isosmotic medium.

Effects of Metabolic Depletion. Metabolic depletion of human red blood cells resulted in the transformation of discocytes into crenated cells (Fig. 7*c*) as previously reported (Nakao, Nakao & Yamazoe, 1960; Weed et al., 1969). This process was reversible upon replenishment of intracellular ATP (Fig. 7*c*, insert). In contrast in the llama, depletion of intracellular ATP to near zero levels (< 0.01 μg/g hemoglobin) did not evoke a change in shape (Fig. 7*d*). Subsequent incubation of the ATP-depleted llama erythrocytes with adenosine resulted in the restoration of over 80% of the intracellular ATP level. These ATP-replenished cells remain essentially elliptical.

Effects of Lysophosphatidylcholine (LPC). Various concentrations of LPC (6, 12, 20 μg/ml) transform human discocytes into echinocytes and sphero-echinocytes as reported previously (Deuticke, 1968; Marikovsky et al., 1976). Incubation of human red cells in 20 μg/ml of LPC at 25 °C produces sphero-echinocytes (Fig. 7*e*); similar treatment of llama erythrocytes did not result in spicules, but rather, in serrations of the perimeters of the llama elliptocytes (Fig. 7*f*). When compared to the pointed spicules of the human sphero-echinocytes, the serrations or scalloping of the llama red cell surface appeared regularly curved and blunt. Although the shape alterations in the llama appeared less drastic, the incorporation of LPC into the membranes per unit of surface at concentration of 20 μg/ml was actually higher in the llama than human. At 25 °C, 1.9×10^{-10} μg of LPC was incorporated per μm^2 of human and 3.6×10^{-10} μg per μm^2 of llama membrane. There was greater degree of incorporation of LPC into both human and llama membranes at 0 °C (3.1×10^{-10} per μm^2 of human and 5.3×10^{-10} per μm^2 of llama membrane). The lytic effect of low temperature incubation with LPC was partial on the human and complete on the llama red cells.

Discussion

Llama erythrocytes differed from human erythrocytes in several interesting ways. They were small elliptical disks. They resisted three treatments which converted human erythrocytes into spiculated forms: incubation in hypertonic media, energy depletion and incubation with lysophosphatidylcholine. We attribute these species differences to the membrane.

We have demonstrated, in the present study, that although the llama erythrocyte has approximately one-third of the human erythrocyte surface area, it contains a similar number of band 3 polypeptides. Thus, the llama membrane has a two and a half to threefold increase in band 3 polypeptide concentration. There is also modest enrichment in sialic acid. In contrast, spectrin (bands 1 and 2) are of the same relative concentration in llama and human membranes. We believe that some of the

differences between human and llama membranes result from the high content of intrinsic protein of the membrane, just as in the camel (Ralston, 1975; Eitan, Aloni & Livne, 1976). The usual concept of the red cell membrane as a bilayer studded with occasional integral proteins gives way to the concept of a close-packed lipid/protein matrix in the llama erythrocyte membranes. A similar high content of proteins in membranes has been found in the gap junctions (Evans & Gurd, 1972), the purple membranes of *Halobacterium halobium* (*see* Osterhelt & Stoeckenius, 1971) and the outer membrane of *E. coli* (Schnaitman, 1970). In almost all cases, curvature and flexibility are reduced and mechanical strength is increased. Several of these high protein membranes show resistance to solubilization by Triton X-100 (Cotman, Levy, Banker & Taylor, 1971; Schnaitman, 1971*a b*) or by other detergents (Emmelot, Feltkamp & Vaz Diaz, 1970; Evans & Gurd, 1972). The resistance of llama erythrocytes to shape transformations by hyperosmotic factors, metabolic depletion and lysophosphatidylcholine may also be related to the high content of intrinsic protein.

The pattern of aqueous extraction of the llama membranes qualitatively resembles that previously seen for the humans (Steck & Yu, 1973). The absence of band 6 in the llama profile may signify a weak attachment which is dissociated during the washing of the ghosts. The fact that the extraction of the peripheral proteins was more complete in the human than the llama ghosts might signify a kinetic effect. For example, the proteins must exit from the ghosts through a single hole (Lieber & Steck, 1982*a*, *b*); this could be small in the llama, hence rate-limiting. It may also be that the affinity of certain llama proteins for the membrane (e.g. bands 1, 2 and 2.1) may be greater than for the human or that their resistance to denaturation is enhanced. In contrast, band 3 and the (sialo)glycoproteins remain membrane-bound through all of the aqueous extractions, consistent with their integration into the bilayer. A similar set of data and interpretation has been presented for the camel erythrocyte (Ralston, 1975, Eitan et al., 1976). Thus, there is no reason to believe that these proteins have a disposition in the llama membrane which is different from that of the human (*see* Steck, 1974).

Topography of Band 3

The data on the llama support the contention that the intramembrane particle population in the protoplasmic leaflet (P-face) is attributable to band 3 (Weinstein, Khodadad & Steck, 1978*a*, *b*; Weinstein, Khodadad & Steck, 1980*a*). The numbers of band 3 polypeptides per cell are similar in llama and human. Total numbers of P-face particles per cell are also nearly identical in the two species, if correction is made for dimensional distortions introduced by the scanning electron-microscopy preparative techniques. Glutaraldehyde fixation and air drying reduced human erythrocyte diameters approximately 16%, from 8.07 ± 0.43 (SD) μm in the unfixed hydrated state (Canham & Burton, 1968), to 6.80 ± 0.4 (SD) μm in this study. Correspondingly, there is an approximately 30% reduction in surface area in our scanning electron-microscopy preparations of intact erythrocytes. Assuming that we have underestimated the llama erythrocyte surface area by approximately 30% as well, the corrected number of P-face particles per llama erythrocyte is $2.34 \times 10^5 / 0.7 = 3.34 \times 10^5$ which is equivalent to the numbers of P-face particles per human erythrocyte. In both llama and human the band 3 protein is probably associated in the membrane predominantly as a tetramer (Weinstein, Khodadad & Steck, 1980*a*, *b*). The major difference between these species is the increased concentration of band 3 per unit area of llama erythrocyte membrane.

Physiological Considerations

The major function of band 3 is to mediate anion exchange (primarily Cl^- and HCO_3^-) and thus facilitate CO_2 transport from the tissues to the lungs. The rather high level of band 3 might then reflect a particular need for anion transport capacity in the llama. Band 3 confers the anion exchange capacity of the erythrocyte membrane (Cabantchik & Rothstein, 1974; *see* Cabantchik, Knauf & Rothstein, 1978). A titration of anion transport sites shows a similar number in llama and human; furthermore, the anion transport capacity is similar in human and llama cells (R.B. Gunn and O. Frohlich, *personal communication*). It is interesting that the llama has increased its anion exchange capacity by adding more sites, even though this crowds the bilayer to nearly a maximum density, rather than by increasing the maximum velocity of each site. This suggests that the transporter may be functioning at its maximum in both human and llama erythrocytes.

Concluding Remarks

In conclusion, we have found the llama erythrocyte membrane to be the homologue of the human, composed of corresponding parts. The major proteins have a similar size and disposition, implying

related function. On the other hand, the llama has a higher concentration of integral protein per unit area of membrane which may affect membrane dissolution *in vitro* and could alter its physiological properties as well. All of the distinctive properties found in the llama seem to correspond to a similar pattern in a related species, the camel (Ralston, 1975; Eitan et al., 1976), suggesting that these changes are not adventitious but represent an evolved specialization whose functional significance remains to be defined.

We thank Dr. Theodore L. Steck for his encouragement, many useful suggestions and critical reading of the manuscript. We are grateful to Dr. Yvonne Lange for cholesterol and phospholipid determinations and measurements on lysophosphatidylcholine uptake, and to Drs. Frank H. Wright and Janis E. Ott and the staff of Chicago Zoological Park and Lamb's Farm for samples of llama blood. The expert technical assistance of Mr. James Walsh, Ms. Benita Ramos and Mr. William Leonard is appreciated. We thank Mr. Kenneth R. Groh for his assistance in ATP determinations and the Division of Biological and Medical Research at Argonne National Laboratories for the use of the Farrand Mark IV fluorometer. We thank Mr. Jian Khodadad for his enthusiastic help in the preparation of the manuscript.

This work was supported by a grant from the Chicago Heart Association #A79–46 and funds from the Otho Sprague Memorial Institute.

Preliminary reports on various aspects of this work were presented at the Annual Meetings of the American Society for Cell Biology, November 1980, Cincinnati, Ohio and November 1981, Anaheim, California, the Federation of American Societies of Experimental Biologists, April, 1981, Atlanta, Georgia, and the American Association of Anatomists, April 1982, Indianapolis, Indiana.

References

Ames, B.N. 1966. Assay of inorganic phosphate, total phosphate and phosphatases. *Methods Enzymol.* **8**:115–118

Cabantchik, Z.I., Knauf, P.A., Rothstein, A. 1978. The anion transport system of red blood cells. The role of membrane proteins evaluated by the use of probes. *Biochim. Biophys. Acta* **515**:239–302

Cabantchik, Z.I., Rothstein, A. 1974. Membrane proteins related to anion permeability of human red blood cells. I. Localization of disulfonic stilbene derivatives binding sites in proteins involved in permeation. *J. Membrane Biol.* **15**:207–226

Canham, P.B., Burton, A.C. 1968. Distribution of size and shape in populations of normal human red cells. *Circ. Res.* **22**:405–422

Considine, D.M. 1976. Van Nostrand's Scientific Encyclopedia. Von Nostrand Reinold Company. Fifth edition, p. 940. New York, Cincinnati, Atlanta, Dallas, San Francisco, London, Melbourne, Toronto

Cotman, C.W., Levy, W., Banker, G., Taylor, D. 1971. An ultrastructural and chemical analysis of the effect of Triton X-100 on synaptic plasma membranes. *Biochim. Biophys. Acta* **249**:406–418

Deuticke, B. 1968. Transformation and restoration of the biconcave shape of human erythrocyte induced by amphipathic agents and changes of ionic environment *Biochim. Biophys. Acta* **163**:494–500

Dodge, T.J., Mitchell, C., Hanahan, D.J. 1963. The preparation and chemical characteristics of hemoglobin free ghosts of human erythrocytes. *Arch. Biochem. Biophys.* **100**:119–130

Eitan, A., Aloni, B., Livne, A. 1976. Unique properties of the camel erythrocyte membrane. II. Organization of membrane proteins. *Biochim. Biophys. Acta* **426**:647–658

Emmelot, P., Feltkamp, C.A., Vaz Diaz, H. 1970. Studies on plasma membranes. XII. Fractionation of the ATPase of deoxycholate-solubilized rat liver and hepatoma plasma membranes and the morphological appearance of the preparations. *Biochim. Biophys. Acta* **211**:43–55

Evans, W.H., Gurd, J.W. 1972. Preparation and properties of nexuses and lipid enriched vesicles from mouse liver plasma membranes. *Biochem. J.* **128**:691–700

Fairbanks, G., Steck, T.L., Wallach, D.F. 1971. Electrophoretic analysis of the major polypeptides of the human erythrocyte membrane. *Biochemistry* **10**:2606–2617

Folch, J., Lees, M., Sloane-Stanley, G.H. 1957. A simple method for isolation and purification of total lipids from animal tissues *J. Biol. Chem.* **226**:497–509

Gomori, G. 1942. A modification of the colorimetric phosphorus determination for use with the photoelectric colorimeter. *J. Lab. Clin. Med.* **27**:955–960

Guidotti, G. 1972. Membrane proteins. *Annu. Rev. Biochem.* **41**:731–752

Kant, J.A., Steck, T.L. 1973. Specificity in the association of glyceraldehyde-3-phophate dehydrogenase with isolated human erythrocyte membranes. *J. Biol. Chem.* **248**:8457–8464

Khodadad, J.K., Weinstein, R.S. 1980. Comparative studies on the membranes of llama and human erythrocytes. *Proc. Electron Micros. Soc. America,* Thirty Eighth Annual Meeting, pp. 788–789

Lange, Y., Slayton, J.M. 1982. Interaction of cholesterol and lysophosphatidylcholine in determining red cell shape. *J. Lipid Res.* **23**:1121–1127

Lieber, M.R., Steck, T.L. 1982*a*. Description of the holes in human erythrocyte membrane ghosts. *J. Biol. Chem.* **257**:11651–11659

Lieber, M.R., Steck, T.L. 1982*b*. Dynamics of the holes in human erythrocyte membrane ghosts. *J. Biol. Chem.* **257**:11660–11666

Livne, A., Kuiper, P.J.C. 1973. Unique properties of the camel erythrocyte membrane. *Biochim. Biophys. Acta* **318**:41–49

Lowry, O.H., Rosebrough, N.J., Farr, A.L., Randall, R.J. 1951. Protein measurement with the folin phenol reagent. *J. Biol. Chem.* **193**:265–275

Margaritis, L.H., Elgsaeter, A., Branton, D. 1977. Rotary replication for freeze-etching. *J. Cell Biol.* **72**:47–56

Marikovsky, Y., Brown, C.S., Weinstein, R.S., Wortis, H.H. 1976. Effects of lysolecithin on the surface properties of human erythrocytes. *Exp. Cell Res.* **98**:313–324

Marikovsky, Y., Khodadad, J.K., Weinstein, R.S. 1978. Influence of red cell shape on surface charge topography. *Exp. Cell Res.* **116**:191–197

Moor, H., Mühlethaler, K. 1963. Fine structure in frozen-etched yeast cells. *J. Cell Biol.* **17**:609–628

Nakao, M., Nakao, T., Yamazoe, S. 1960. Adenosine triphosphate and maintenance of shape of the human red cells. *Nature, New Biol.* **187**:945–946

Osterhelt, D., Stoeckenius, W. 1971. Rhodopsin-like protein from the purple membrane of *Halobacterium halobium*. *Nature, New Biol.* **233**:149–152

Parekh, A.C., Jung, D.H. 1970. Cholesterol determination with ferric acetate-uranium acetate and sulfuric acid-ferrous sulfate reagents. *Anal. Chem.* **42**:1423–1427

Perk, K. 1963. The camel erythrocyte. *Nature, New Biol.* **200**:272–273

Perk, K., Frei, Y.F., Herz, A. 1964. Osmotic fragility of red

blood cells of young and mature domestic and laboratory animals. *Am. J. Vet. Res.* **25**:1241–1248

Ponder, E. 1948. Shape changes unaccompanied by volume changes. *In:* Hemolysis and Related Phenomena. pp. 10–26. Grune & Stratton, editors, New York

Ralston, G.B. 1975. Proteins of the camel erythrocyte membrane. *Biochim. Biophys. Acta* **401**:83–94

Reynafarje, C., Faura, J., Villavicencio, D., Curaca, A., Reynafarje, B., Oyola, L., Contreras, L., Vallenas, E., Faura, A. 1975. Oxygen transport of hemoglobin in high-altitude animals (*Camelidae*). *J. Appl. Physiol.* **38**:806–810

Robertson, J.D. 1959. The ultrastructure of cell membranes and their derivatives. *Biochem. Soc. Symp.* **16**:3–43

Schmid-Schonbein, H., Wells, F. 1969. Fluid drop-like transition of erythrocytes under shear. *Science* **165**:288–291

Schnaitman, C.A. 1970. Protein composition of the cell wall and cytoplasmic membranes of *Escherichia coli*. *J. Bacteriol.* **104**:890–901

Schnaitman, C.A. 1971*a*. Solubilization of the cytoplasmic membrane of *Eschrichia coli* in Triton X-100. *J. Bacteriol.* **108**:545–552

Schnaitman, C.A. 1971*b*. Effect of ethylendiaminetetraacetic acid, Triton X-100, and lysoszyme on the morphology and chemical composition of isolated cell walls of *Escherichia coli*. *J. Bacteriol.* **108**:553–563

Smith, J.E., Mohandas, N., Shohet, S.B. 1979. Variability in erythrocyte deformability among various mammals. *Am. J. Physiol.* **236**:H725–730

Steck, T.L. 1974. The organization of proteins in the human red blood cell membrane. *J. Cell Biol.* **62**:1–19

Steck, T.L. 1978. The band 3 protein of the human red cell membrane: A review. *J. Supramol. Struct.* **8**:311–324

Steck, T.L., Yu, J. 1973. Selective solubilization of proteins from red blood cell membranes by protein perturbants. *J. Supramol. Struct.* **1**:220–232

Strehler, B.L., McElroy, W.D. 1968. Assay of adenosine triphosphate. *Methods Enzymol.* **3**:871–873

Tischer, I., Peters, D. 1965. Methode zur bestimmung des salinsauregehaltes von erythrocyten und haemoglobinhaltigen wasserigen sialinsaurelosungen. *Zentralbl. Bakteriol. Parasitenkd. Infektionskr. Hyg., Abt. 1:* Orig. **195**:408–515

Warren, L. 1959. The thiobarbituric acid assay of sialic acids. *J. Biol. Chem.* **234**:1971–1975

Weed, R.I., La Celle, P.L., Merrill, D.W. 1969. Metabolic dependences of red cell deformability. *J. Clin. Invest.* **48**:795–809

Weinstein, R.S., Khodadad, J.K., Steck, T.L. 1978*a*. Ultrastructural characterization of proteins at the natural surfaces of the red cell membrane. *Prog. Clin. Biol. Res.* **21**:413–427

Weinstein, R.S., Khodadad, J.K., Steck, T.L. 1978*b*. Fine structure of the band 3 protein in human red cell membranes. Freeze-fracture studies. *J. Supramol. Struct.* **8**:325–335

Weinstein, R.S., Khodadad, J.K., Steck, T.L. 1980*a*. The band 3 protein particle of the human red blood cells. *In:* Membrane Transport in Erythrocytes. U.V. Lassen, H.H. Ussing and J.O. Weith, editors. pp. 35–50. Munksgaard, Copenhagen

Weinstein, R.S., Khodadad, J.K., Steck, T.L. 1980*b*. Band 3 protein is a tetramer in the human red cell membrane. *J. Cell Biol.* **87**:209a

Yagil, R., Sod-Moriah, U.A., Meyerstein, N. 1974. Dehydration and camel blood. II. Shape, size, and concentration of red blood cells. *Am. J. Physiol.* **226**:301–304

Yu, J., Fischman, D.A., Steck, T.L. 1973. Selective solubilization of proteins and phospholipids from red blood cell membranes by non-ionic detergents. *J. Supramol. Struct.* **1**:233–244

Yu, J., Steck, T.L. 1975. Associations of band 3, the predominant polypeptide of the human erythrocyte membrane. *J. Biol. Chem.* **250**:9176–9184

Received 25 May 1982; revised 8 September 1982